



FAU Institutional Repository

<http://purl.fcla.edu/fau/fauir>

This paper was submitted by the faculty of [FAU's Harbor Branch Oceanographic Institute](#).

Notice: ©1999 IEEE. Personal use of this material is permitted. Permission from IEEE must be obtained for all other uses, in any current or future media, including reprinting/republishing this material for advertising or promotional purposes, creating new collective works, for resale or redistribution to servers or lists, or reuse of any copyrighted component of this work in other works.

This manuscript is available at <http://ieeexplore.ieee.org/> and may be cited as: Caimi, F. M., Bailey, B. C., & Blatt, J. H. (1999). Undersea object detection and recognition: the use of spatially and temporally varying coherent illumination. *Oceans'99 MTS/IEEE: Riding the crest into the 21st century*. (Vol. 3, pp. 1474-1479). Washington, DC: Oceans'99 MTS/IEEE Conference Committee.
doi:10.1109/OCEANS.1999.800211

Undersea Object Detection and Recognition: The Use of Spatially and Temporally Varying Coherent Illumination

Frank M. Caimi¹

Department of Electrical Engineering
Florida Institute of Technology
150 W University Blvd.
Melbourne, Florida 32901

Bernard C. Bailey and Joel H. Blatt
Department of Physics and Space Sciences
Florida Institute of Technology
150 W University Blvd.
Melbourne, Florida 32901

Abstract: Increased optical range of target detection and recognition is always a problem in the marine environment. The inherent optical properties of light absorption and scattering in water limit both radiative and information transfer for image formation. These limits are further restricted by suspended particulate matter scattering. Near the surface in peak daylight conditions, the intense background scattered light makes for an extremely difficult job of object detection due to contrast washout. In any conventional underwater imaging system design, these limitations are either difficult or seemingly impossible to surmount. Methods for the formation of images in scattering media generally rely upon temporal or spatial methodologies. Some interesting designs have been developed in an attempt to circumvent or overcome the scattering problem. Time gating is a temporal example of image formation whereby a light source is time pulse projected toward a target and the detector is time gated to accept image-forming illumination from a specific range. To be successful at eliminating much of the backscatter, this method requires exacting range information and loses the simplicity of a continuous light source. Holography is one example of an image formation method requiring specific spatial relationships, i.e. mutual coherence between a reference beam and a signal beam. The coherence allows the formation of an interference pattern that carries the signal information on a "spatial carrier". In order for the method to be of use, the medium in which the beams are carried must preserve the coherence or phase spatially across the beams and in relation to the reference beam. In water, the distance over which the phase may be preserved is dependent upon many factors, including turbulence induced refractive index variations, thermal gradient structure, and relative motion. If pathlength differences exceed the temporal coherence length of the beam, interference is not obtained and the method breaks down. Generally, the demands of maintaining a spatially coherent beam at optical frequencies is difficult over long range thereby limiting the usefulness of the technique for image formation in turbid media. A paper submitted by the authors at the OCEANS '98 Conference describes a variation of the spatial interferometric technique that relies upon projected spatial

gratings with subsequent detection against a quasi-coherent return signal. The method is advantageous in not requiring temporal coherence between reference and signal beams and may use a continuous illumination source. Coherency of the spatial beam allows detection of the direct return, while scattered light appears as a noncoherent noise term. The theoretical foundation of the method and the initial results for turbid media were developed. This paper will present the latest ongoing research results.

I. INTRODUCTION

Most laser imaging systems are designed to reduce the effects of scattering on the produced image improving image visibility in near shore water conditions. Synchronous scan systems minimize the common volume occupied by laser illumination and the detector field-of-view [1]. LIDAR systems time gate the receiver aperture to eliminate relatively intense backscatter originating from the water while allowing the return from the target to be detected [2]. Both systems provide a specific set of advantages, but neither normally utilize coherent detection techniques to improve performance. In addition, the systems produce reflectance maps of the scene being illuminated and are not particularly sensitive to object contour, shape, or surface texture.

Recently, several laboratories have demonstrated the use of temporal modulation and subsequent synchronous detection to improve imaging of subsurface objects in shallow water environments [11]. The technique allows for the extraction of the signal reflected from the target/object via a synchronous detection technique that is well known in signal detection theory. The advantage of the approach is that the signal return from the target is coherent with the transmitted waveform while the return produced from scattering is quasicohherent and represents noise. The idea is to achieve "processing gain" via correlation of the transmitted and received signals against a "noise" background.

¹ Author is also affiliated with Harbor Branch Oceanographic Institution, Ft. Pierce, Fl.

This technique was proposed by the authors as well, and may provide needed improvement in the detection of low contrast targets.

Unfortunately, real world scenes often exhibit nearly identical reflectance over a two dimensional cross section especially if the target reflectivity matches the background, making difficult the task of interpreting depth cues, especially in turbid water at maximum range where the signal-to-noise ratio is low. Observation of undersea objects with 2-D imaging devices requires sufficient contrast at spatial frequencies corresponding to the characteristic features on the object surface or, at a minimum, shape information consistent with a feature database. Features distributed in the range or depth dimension are often subject to misinterpretation since reflectance information alone does not necessarily provide an adequate feature set for reliable detection or identification. Additional information useful for object identification and characterization can be obtained by creating a range map or depth contours, and methods have been devised to obtain shape, velocity, and position information using intensity gradient cues observed in the scene as a result of illumination from natural or artificial light sources [3, 4].

Range or depth information is available from LIDAR, structured illumination (e.g. via triangulation), and interferometric system approaches. The resolution achievable is dependent upon the laser pulsewidth, system geometry, and environmental parameters in each case. Although LIDAR and triangulation [5] methods have received a significant amount of attention, they do not offer the potential advantages of an interferometric approach. Interferometric systems [6, 7] can be classified as temporally or spatially modulated types. There are several recent reports using temporal modulation to improve image quality and to acquire range information, but few using spatial coherency (modulation). Holography has also been tried and functions over very short distances where both temporal and spatial coherency remains relatively unperturbed by the properties of the medium.

An alternative approach using spatially modulated or coded waveforms has been proposed [7, 8] offering an intermediate solution to obtaining additional feature information, and utilizing novel optical techniques and signal processing algorithms for object classification, feature extraction, and image restoration with minimum a-priori information.

In an earlier paper [8], the background, definitions, theoretical development and implementation methodologies were introduced. In this paper, some of the theoretical computer modeling and an early qualitative experiment are introduced.

II. TRANSMISSION MODEL

Much of the transmission model used has been previously derived by other authors. According to Mertens [9], the spread function due to refractive deterioration along the transmission path closely resembles the Gaussian curve.

The standard deviation σ is used as a measure of spreading and the rms value of observed spreading is set equal to σ . The modulation transfer function (MTF) corresponding to the refractive deterioration on the direct image is given as and exponential dependence related to σ and the angular frequency. Recent models [10] suggest MTF remains relatively constant over a large angular frequency range above some low frequency limit. These models are in agreement with the suggestion and results in this paper showing that high spatial frequency content can be used for detection against the scattered light field even if large angular frequencies are used.

Using the conventional model of Mertens, the resulting MTF can be approximated as

$$T_P = \begin{cases} 1 & \omega \cong 0 \\ C \exp(-0.5 \cdot \sigma^2 \cdot \omega^2) & \omega > 0, \end{cases} \quad (1)$$

where C represents direct image scattering attenuation. Experimental values of σ are:

$$\sigma \cong 1.9 \times 10^{-4} \text{ rad, giving}$$

$$T_R = \exp(-0.692 \times 10^{-6} f^2), \quad (2)$$

where f is the spatial frequency in cycles per radian. This model initially addresses only the effect of the refractive deterioration or transmittance T_R .

Target illumination from a monochromatic source at normal incidence and distance r is considered to be a sum of a direct component, E_D , and a forward-scattered component, E_S . We assume that the target is illuminated by vertical light fringes emanating from a Michaelson Interferometer and that they are essentially parallel as in Fig. 12. After a beam expander, the fringes maintain a uniform separation and appear slightly divergent. However, for the distances being studied, this model assumes parallel illumination and simplifies the illuminance calculations by disregarding all terms in $E_S(r)$ involving the scattering phase function. To simulate vertical fringes, the intensity I is modified by a cosine function which allows a normalized intensity to range from 0 to 1. To affect forward scattering in each transmission fringe, the refractive deterioration MTF factor is applied directly to the cosine function in the E_S term. The total illuminance at the target is the sum of the terms:

$$E(r) = E_D(r) + E_S(r). \quad (3)$$

The difference between the target illuminance and the background illuminance at the detector a distance r from the target can be represented by a luminance (or radiance) term

$$B_d = E(r) (R_t - R_b) e^{-cr}/\pi, \quad (4)$$

where R_t and R_b are target and background reflectivity.

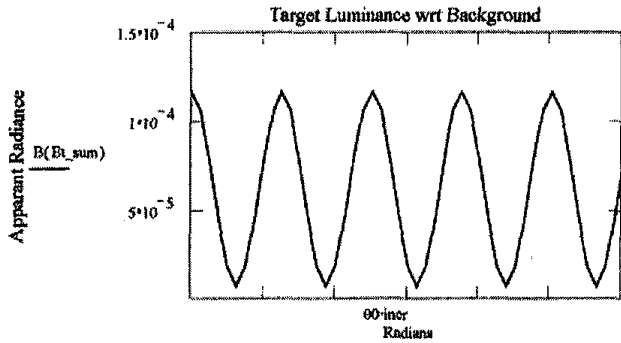


Fig. 1: Structured Illumination Transmission model example.

The above graph is a representative result of the transmission model in Mathcad with $r = 4.5$ meters, $c = 0.33$, a target illuminated spatial frequency of 1 cm/cycle, and source intensity normalized.

III. BACKSCATTER MODEL

A MTF backscatter model modified for spatially modulated illumination (SMI) has been recently developed also using the standard model as outlined by Mertens, integrating over the common volume intersected by source, target and detector.

The total illuminance is the sum of direct and backscatter terms:

$$E(r) = E_D(r) + E_{BS}(r) \quad (5)$$

where

$$E_D(r) := \frac{I \cdot e^{-cr}}{r^2}$$

$$E_{BS}(r) := \frac{2.5 \cdot I \cdot k \cdot e^{-kr}}{4 \pi r} \quad (6)$$

The apparent radiance is an integral between r_i and r_t , the two end points of the common volume along the line of sight:

$$B(r) := \int_{r_i}^{r_t} s \cdot E(r) \cdot e^{-kr} dr \quad (7)$$

where s is the average backscatter coefficient at the detector to illuminator offset angle.

In all figures in this section and in the next, w is the spatial frequency of the SMI, r is distance between source and target,

and c is the average backscatter coefficient at detector to illuminator offset angle.

Figures 2 and 3 below show comparative results between SMI and conventional lighting using the same parameters as in the transmission model. The figures indicate a backscatter apparent radiance relative to source output. There are two important features to note: 1) SMI backscatter is significantly less than from a conventional source; 2) There is little to no structure within the SMI backscatter, especially as spatial frequency increases.

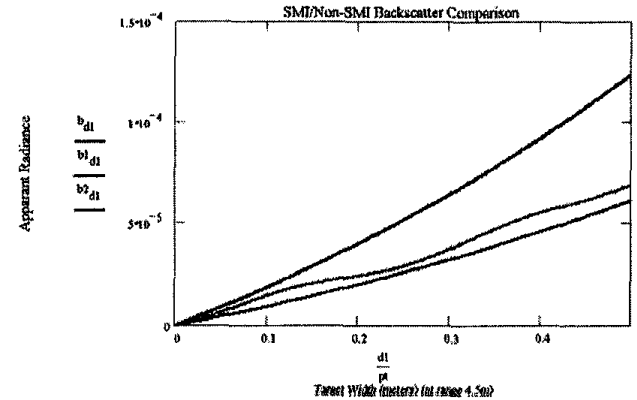


Fig. 2: b_{d1} = SAH Backscatter; b_{l_d1} = Conventional Backscatter; b_{2_d1} = 1/2 Conventional Backscatter; $w = 0.25$ m/cycle, $r = 4.5$ meters, $c = 0.33$

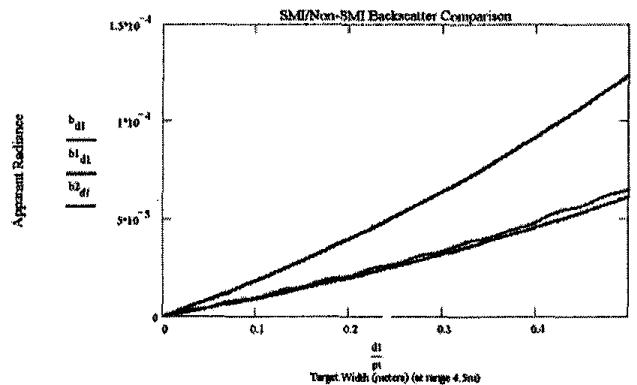


Fig. 3: b_{d1} = SMI Backscatter; b_{l_d1} = Conventional Backscatter; b_{2_d1} = 1/2 Conventional Backscatter; $w = 0.05$ m/cycle, $r = 4.5$ meters, $c = 0.33$

IV. COMBINED SMI MODEL

Figures 4 through 6 show a comparison of transmitted and backscattered apparent radiance at varying spatial frequency and target range. The lack of structure in the backscatter as compared to the SMI is quite evident. Figures 7 through 11 show the sum of transmitted and backscattered apparent

radiance at varying spatial frequency and target range. The most important feature to note in these figures is that the modulation remains in the received transmission to the edge of detection.

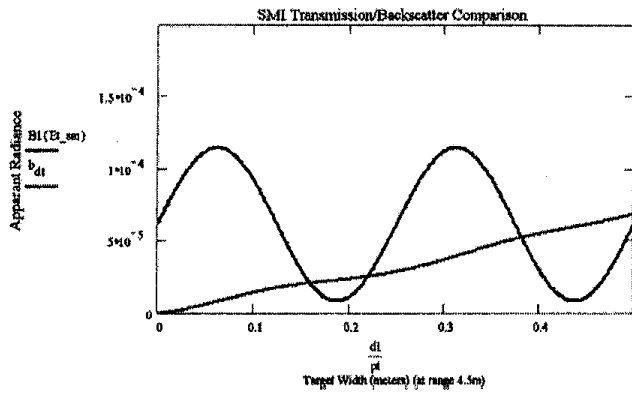


Fig. 4: b_{d1} = SIM Backscatter; $B1(Et_{sm})$ = SMI Transmission; b_{d1} = SMI Backscatter; $w = 0.25$ m/cycle, $r = 4.5$ meters, $c = 0.33$

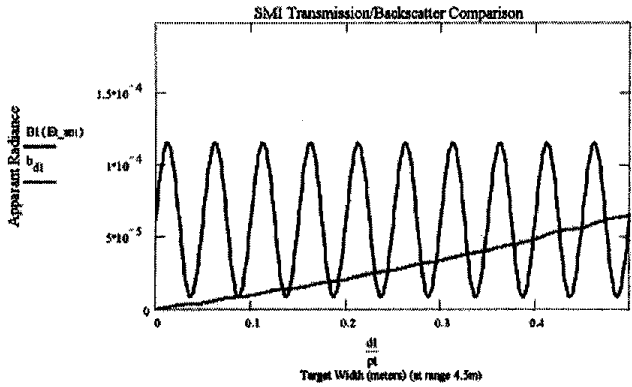


Fig. 5: b_{d1} = SMI Backscatter; $B1(Et_{sm})$ = SMI Transmission; b_{d1} = SMI Backscatter; $w = 0.05$ m/cycle, $r = 4.5$ meters, $c = 0.33$

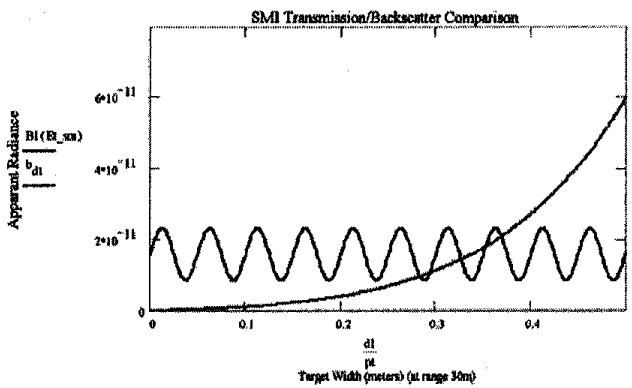


Fig. 6: b_{d1} = SMI Backscatter; $B1(Et_{sm})$ = SMI Transmission; b_{d1} = SMI Backscatter; $w = 0.05$ m/cycle, $r = 30$ meters, $c = 0.33$

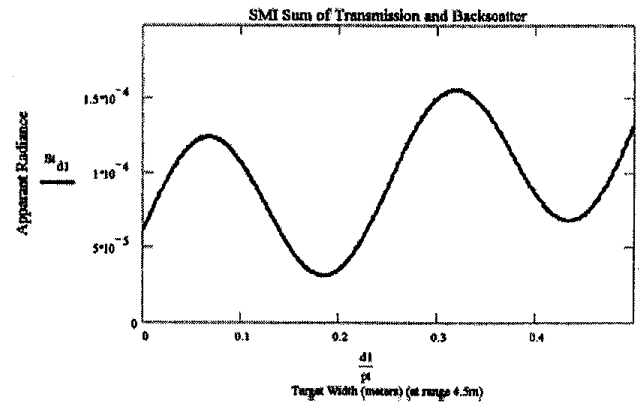


Fig. 7: Bt_{d1} = SMI Sum of Transmission and Backscatter; $w = 0.25$ m/cycle, $r = 4.5$ meters, $c = 0.33$

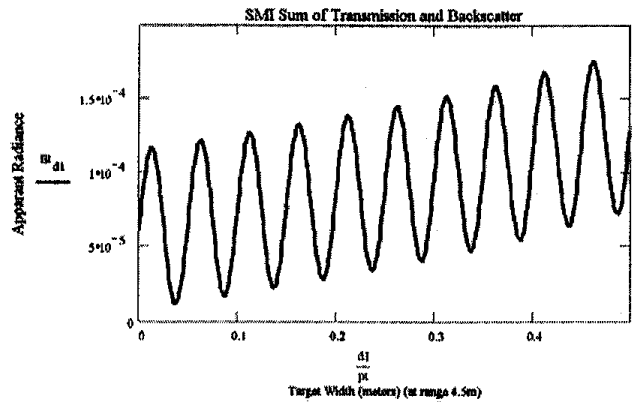


Fig. 8: Bt_{d1} = SMI Sum of Transmission and Backscatter; $w = 0.05$ m/cycle, $r = 4.5$ meters, $c = 0.33$

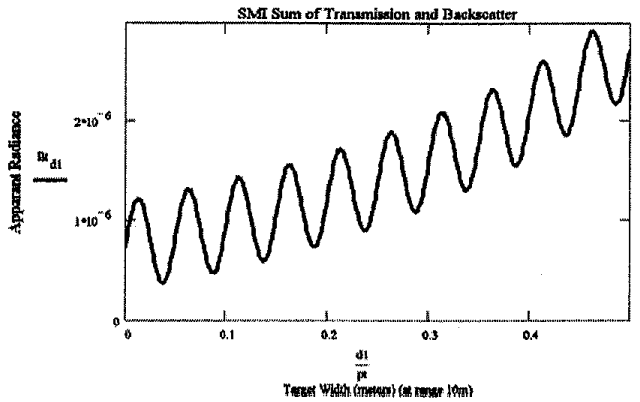


Fig. 9: Bt_{d1} = SMI Sum of Transmission and Backscatter; $w = 0.05$ m/cycle, $r = 10$ meters, $c = 0.33$

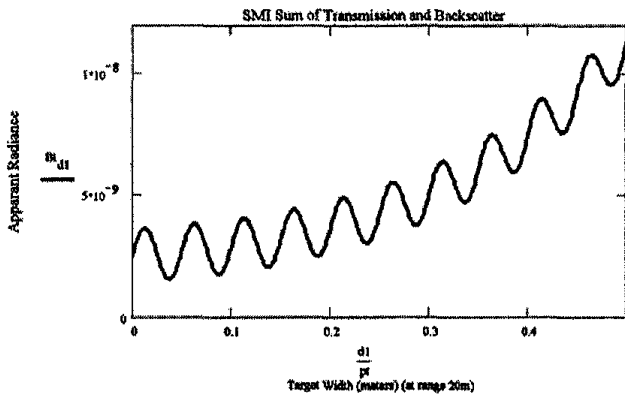


Fig. 10: B_{d1} = SMI Sum of Transmission and Backscatter; $w = 0.05$ m/cycle, $r = 20$ meters, $c = 0.33$

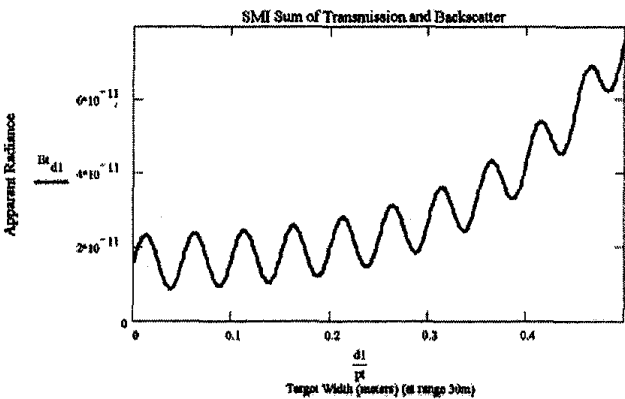


Fig. 11: B_{d1} = SMI Sum of Transmission and Backscatter; $w = 0.05$ m/cycle, $r = 30$ meters, $c = 0.33$

V. INITIAL EXPERIMENT

An experiment was devised using a variable frequency illumination source and highly turbid medium to investigate the presence of spatially modulated backscattered light at various angular frequencies (Figure 12).

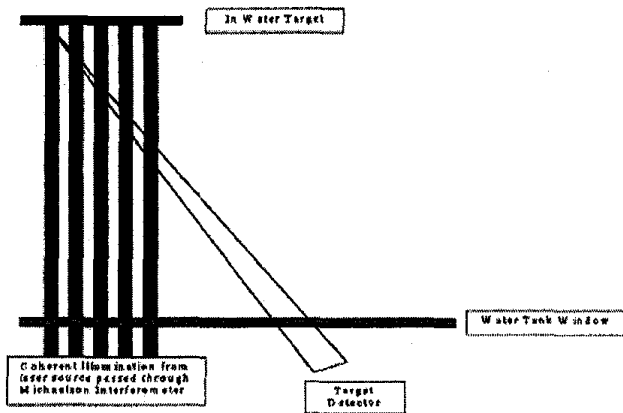


Figure 12. Experimental setup for proof of principle.

The proposed detection method for discriminating the spatially modulated returns from the target against the veiling illumination due to scatter requires the scattered light field to exhibit little or no observable modulation. The experiment was designed to observe the transmission and backscatter of a spatially variant (structured) illumination source created by a portable Michelson interferometer and 1 to 2 watt argon ion laser operating at 514 nm. The interferometer was adjusted to provide adjustable spatial frequency vertical fringes at the side entrance window of a 4.5-meter diameter tank of water.

Figures 13-15 are photographs of the modulated beam from different vantage points. As the model predicts, there is no observable structure evident in the backscatter (left side of Fig. 13) when viewing the beam fringes from the side. The fringes are lost as the viewing angle is changed slightly from a look direction parallel to beam propagation direction. The fringes are observed, however, at the rear wall of the tank (i.e. at the target plane). Figs. 14 and 15 show a low contrast image produced by a target illuminated with low and high spatial frequency structure, respectively. Only the shadows provide an indication of the presence of a raised surface against the tank wall. Fringe structure is observable however, and is modulated spatially by the variation of object profile in the beam propagation direction. Detection of these variations via spatial correlation methods can then provide a means of detection for otherwise featureless images in high turbidity environments.

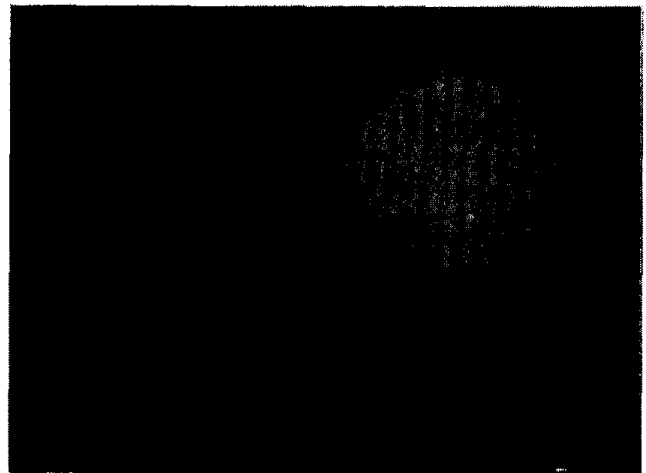


Fig. 13: View of reflection from rear of tank as well as crossbeam backscatter in foreground. Structure is not visible in scatter normal to fringes.

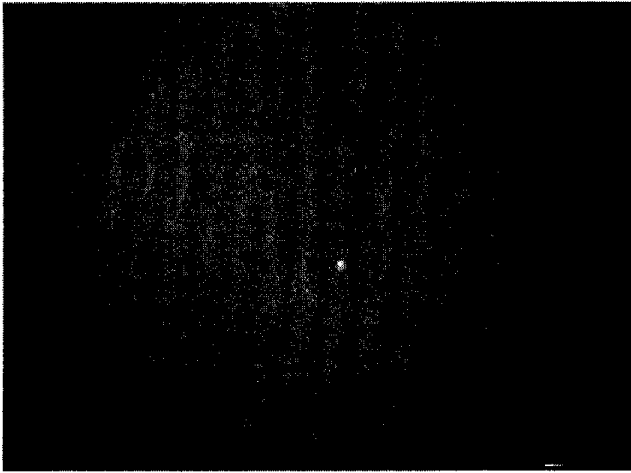


Fig. 14: View of low contrast target against tank wall with low spatial frequency illumination.

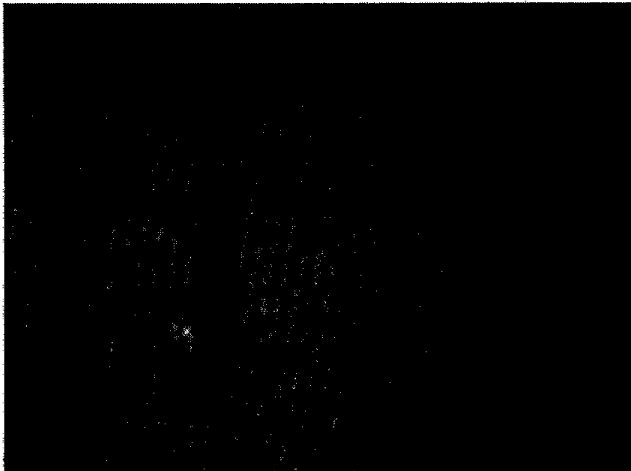


Fig. 15: View of low contrast target slightly away from tank wall with high spatial frequency illumination.

V. CONCLUSIONS

A spatially variant modulation method using a laser has been proposed and demonstrated for use in detection of low contrast targets in turbid water conditions. The method has the advantage of using pulsed illumination (range gating) in conjunction with a spatial profiling method that may also be synchronously demodulated against the veiling luminance due to scattering. The viability of the physical approach has been verified to first order by experiment and by model results.

The design and implementation of discriminant detection methodology is a subject of current work. It is expected that specific signatures due to target shape may be detected or identified by standard methods used for target recognition once the spatial profile is converted to an electrical signal.

Direct optical methods for correlation are more difficult to implement. A combined technique for converting the spatial profile to a temporally variant signature is being investigated. Wide/Narrow and Narrow/Wide techniques are possible for source/detector fields-of-view. Additional work is required to assess the advantages gained in relation to existing imaging methods.

ACKNOWLEDGMENTS

The authors wish to thank the Atlantic Foundation for partial support of this work. This is HBOI contribution number 1309.

REFERENCES

1. Funk, C. J., Bryant, S. B., and Heckman, P., *Handbook of Underwater Imaging System design*, Ocean Technology Dept., NUSC, 1972.
2. Heckman, P., and Hodgson, "Underwater Optical Range Gating", *IEEE Journal of Quantum Electronics*, QE-3, 11, Nov. 1967
3. Horn, B. K. P., *Robot Vision*, MIT Press, 1986.
4. Yu, C., and F. M. Caimi, "Determination of Horizontal Motion through Optical Flow Computations", submitted *IEEE J Ocean Engineering*, 1994.
5. Caimi, F. M., J. H. Blatt, B. G. Grossman, et al., "Advanced Underwater Laser Systems for Ranging, Size Estimation, and Profiling", *MTS Journal* 27 (1): 31-41, 1993.
6. Swanson, N. L., "Coherence Loss of Laser Light Propagated through Simulated Coastal Waters", *Proceedings of Ocean Optics XI*, 1750, 1992.
7. Blatt, J. H., F. M. Caimi, and J. Hooker, "Adaptation of Video Moire Techniques to Undersea Mapping and Surface Shape Determination", *Optics and Lasers in Engineering*, March 1991.
8. Caimi, F. M., B. C. Bailey and J. H. Blatt, "Spatial Coherence Methods in Undersea Image Formation and Detection", *OCEANS '96 MTS/IEEE Supplementary Conference Proceedings*, pp. 40-46, 1996
9. Mertens, L. E., *IN-WATER PHOTOGRAPHY Theory and Practice*, Wiley-Interscience Series, 1970.
10. Fournier, G. R., M. Jonasz, "Computer Based Imaging Analysis," *Proc. SPIE*, Denver, July 1999. Paper 3761-09
11. Mullen, V. M., M. Strand, B. Coles, "Modulated Laser Line Scanner for Enhanced Underwater Imaging", *Proc. SPIE*, Denver, July 1999. Paper 3761-01.